Force-induced focal adhesion translocation: effects of force amplitude and frequency

P. J. Mack, M. R. Kaazempur-Mofrad, H. Karcher, R. T. Lee and R. D. Kamm

Am J Physiol Cell Physiol 287:954-962, 2004. First published Jun 9, 2004;
doi:10.1152/ajpcell.00567.2003

Am J Physiol Cell Physiol 287: C954–C962, 2004.
First published June 9, 2004; 10.1152/ajpcell.00567.2003.

Force-induced focal adhesion translocation: effects of force amplitude and frequency

P. J. Mack,[1] M. R. Kaazempur-Mofrad,[1] H. Karcher,[1] R. T. Lee,[2] and R. D. Kamm[1]

[1]*Department of Mechanical Engineering and Biological Engineering Division, Massachusetts Institute of Technology, Cambridge 02139; and* [2]*Department of Medicine, Brigham and Women's Hospital, Harvard Medical School, Boston, Massachusetts 02115*

Submitted 12 December 2003; accepted in final form 3 June 2004

Mack, P. J., M. R. Kaazempur-Mofrad, H. Karcher, R. T. Lee, and R. D. Kamm. Force-induced focal adhesion translocation: effects of force amplitude and frequency. *Am J Physiol Cell Physiol* 287: C954–C962, 2004. First published June 9, 2004; 10.1152/ajpcell.00567.2003.—Vascular endothelial cells rapidly transduce local mechanical forces into biological signals through numerous processes including the activation of focal adhesion sites. To examine the mechanosensing capabilities of these adhesion sites, focal adhesion translocation was monitored over the course of 5 min with GFP-paxillin while applying nN-level magnetic trap shear forces to the cell apex via integrin-linked magnetic beads. A nongraded steady-load threshold for mechanotransduction was established between 0.90 and 1.45 nN. Activation was greatest near the point of forcing (<7.5 μm), indicating that shear forces imposed on the apical cell membrane transmit nonuniformly to the basal cell surface and that focal adhesion sites may function as individual mechanosensors responding to local levels of force. Results from a continuum, viscoelastic finite element model of magnetocytometry that represented experimental focal adhesion attachments provided support for a nonuniform force transmission to basal surface focal adhesion sites. To further understand the role of force transmission on focal adhesion activation and dynamics, sinusoidally varying forces were applied at 0.1, 1.0, 10, and 50 Hz with a 1.45 nN offset and a 2.25 nN maximum. At 10 and 50 Hz, focal adhesion activation did not vary with spatial location, as observed for steady loading, whereas the response was minimized at 1.0 Hz. Furthermore, applying the tyrosine kinase inhibitors genistein and PP2, a specific Src family kinase inhibitor, showed tyrosine kinase signaling has a role in force-induced translocation. These results highlight the mutual importance of force transmission and biochemical signaling in focal adhesion mechanotransduction.

mechanotransduction; endothelial cell; paxillin; viscoelastic model

MECHANOTRANSDUCTION IS AN essential function of the cell, controlling its growth, proliferation, protein synthesis, and gene expression (8, 18). Extensive data exist documenting the cellular responses to external force (15, 41, 44), but less is known about how force affects rapid biological signaling. Although integrins/focal adhesion sites (42), cytoskeleton constituents, G proteins (6), ion channels, intercellular junction proteins, and membrane biomolecules have all been identified as potential mechanosensors (6, 16, 42, 43), we know little about the force level and frequency-dependent thresholds required to initiate mechanotransduction or the role of intracellular force transmission on mechanosensor activation. Biological readouts used to study mechanotransduction range from long-term gene expression and cell morphology changes (8, 26) to rapid variations in intracellular ion concentration and protein activity (8, 26, 42). Morphological and gene expression comparisons provide a robust marker of mechanotransduction, but the response is slow on the scale of hours, and the methods available to measure changes in molecular activity typically require large cell populations. Intracellular calcium concentration changes, on the other hand, provide a rapid biological readout that can be monitored in a single cell (22, 39) but give little information on the location of the mechanosensor that initiates biological signaling.

Fluid shear stress studies have used cell morphology, gene expression, and intracellular calcium concentration changes to show that cells respond differently to time-varying stress. Cells exposed to rapidly fluctuating shear stress environments, generated with turbulent flow, do not align with the direction of flow as do cells exposed to laminar fluid shear stress (10), whereas oscillating fluid shear stress with a low mean positive force does not induce the same gene expression as flow with a high mean positive force (15, 18, 44). Furthermore, ramped levels of laminar fluid shear stress result in graded nitric oxide (29) and intracellular calcium (38) responses. These studies show that the biological response of a cell to mechanical force depends on both the magnitude and time course of applied external force but present little information regarding the physical basis for these observations.

Focal adhesion site remodeling has also been used as a marker of mechanotransduction, which has the advantage of being rapid (occurring in minutes after stimulation) and site specific (14, 30, 37). Integrin signaling is critical in forming and developing focal adhesion sites as well as in recognizing external force by orchestrating mitogen-activated protein kinase activity and stress fiber formation (42). Both external and internal mechanical stress leads to focal adhesion reinforcement via the recruitment and binding of focal adhesion proteins (14). Src family kinase activation and tyrosine phosphorylation both have roles in early focal adhesion-associated mechanosensing (17). Tyrosine phosphorylation of focal adhesion kinase (FAK) assists in the recruitment and binding of focal adhesion proteins by regulating protein-protein interactions in proteins that contain the Src homology 2 (SH2) (32), whereas Src family kinase activation and interaction with FAK initiates tyrosine phosphorylation of paxillin and p130Cas, leading to Rac-dependent focal adhesion turnover and cell migration (12, 34).

Address for reprint requests and other correspondence: R. D. Kamm, 77 Massachusetts Ave., NE47-321, Cambridge, MA 02139 (E-mail: rdkamm@mit.edu).

The costs of publication of this article were defrayed in part by the payment of page charges. The article must therefore be hereby marked "*advertisement*" in accordance with 18 U.S.C. Section 1734 solely to indicate this fact.

Single cells respond to external forces with focal adhesion translocation and protein recruitment, as shown by fluid shear stress acting as a mechanotaxis stimulus to preferentially translocate focal adhesion sites in the direction of shear (30) and entire cell stretch resulting in increased focal adhesion protein recruitment (37). Cells also respond to locally applied mechanical loads, suggesting that individual focal adhesions sense local levels of force. Pico-Newton level forces applied to the apical cell surface result in focal adhesion protein recruitment to the point of load application (14). Conversely, concentrated apical surface loads on the order of 10 nN per focal adhesion site initiate complex formation and protein recruitment along the basal cell surface in regions local to the concentrated load (35). Understanding how cells transmit mechanical forces from the cell apex to basal adhesions is critical for further characterization of focal adhesion mechanosensing.

In the present study, we examine force magnitude and frequency thresholds for transducing local mechanical loads into biological signals through focal adhesion sites. Using a single pole magnetic trap, we delivered a highly controllable local shear force to the apical cell surface and quantified basal surface focal adhesion translocation. Focal adhesion translocation was monitored with GFP-paxillin, a focal adhesion protein that binds to the focal adhesion targeting (FAT) region of FAK. Translocation exhibited a dependence on both the magnitude and frequency of loading, as well as Src family kinase activity and tyrosine phosphorylation, suggesting that focal adhesion mechanotransduction depends on a balance between the local mechanical stress and specific biochemical signals.

MATERIALS AND METHODS

Endothelial cell culture and materials. Bovine aortic endothelial cells (BAEC) were isolated and *passages 3-8* were used. Endothelial cell isolation was verified with an isolectin stain (Alexa Fluor 594; Molecular Probes, Eugene, OR) by fixing the BAEC in 4% paraformaldehyde for 10 min at room temperature, blocking with 5% BSA for 30 min at room temperature, and incubating at 37°C for 10 min in 1 mg/ml isolectin (neutral pH aqueous buffer). Cells were cultured in DMEM (Cambrex, East Rutherford, NJ) supplemented with 10% FCS and 1% penicillin/streptomycin. Before BAEC plating, 22-mm glass cell culture dishes (WillCo Wells, Amsterdam, The Netherlands) were coated overnight at 4°C with 2 μg/ml fibronectin (cat. no. 33016–023; Invitrogen, Carlsbad, CA) in PBS. BAEC were plated on the fibronectin-coated glass culture dishes in 2 ml DMEM supplemented with antibiotics and 10% FCS at a density of ~100,000 cells/dish. The plated cells were incubated overnight at 37°C.

On reaching ~70% confluence, the BAEC were transiently transfected with the GFP-paxillin vector (gift of K. Yamada, National Institutes of Health, Bethesda, MD) using FuGene6 (Roche, Indianapolis, IN) with a 3:1 transfection reagent (μl)-to-DNA (μg) ratio. Western blot analysis with anti-paxillin (RDI, Flanders, NJ) and anti-GFP (Sigma, St. Louis, MO) monoclonals verified the expression of GFP-paxillin 24 h posttransfection. After incubating at 37°C for 24 h, the medium was exchanged for fresh DMEM, containing 10% FCS, antibiotics, and a suspension of 4.5-μm diameter fibronectin-coated magnetic beads (Dynabeads M-450; Dynal Biotech, Lake Success, NY). The final bead concentration was ~1.6×10^6 beads/dish. BAEC were given a 60-min incubation period at 37°C to allow bead attachment to the cell surface. Src family kinase and tyrosine kinase inhibition was achieved by applying 10 μM PP2 (Calbiochem, La Jolla, CA) or 100 μM genistein (Calbiochem) during the 60 min magnetic bead attachment incubation period at 37°C.

Fluorescent microscopy. Cells were imaged at ×60 magnification with an inverted light microscope (model IX-70; Olympus, Melville, NY) equipped with a water-immersion objective and temperature control plate and recorded with a digital camera (CoolSNAP; Roper Scientific MASD, San Diego, CA). Subconfluent cells expressing GFP-paxillin and binding a single magnetic bead were selected for experimentation. After locating a cell that met the experimental criteria, the magnetic trap was positioned 75 μm from the magnetic bead and lowered to the bead plane. A control sequence of fluorescent images was first obtained by imaging at $t = 0$, 1, 3, and 5 min. After the control sequence, an external forcing function was applied and the cells were again imaged at $t = 1$, 3, and 5 min. The control image at $t = 5$ min was used for the $t = 0$ min forcing sequence image. To ensure basal surface imaging, both the control and forcing function images were recorded as an image stack by scanning vertically 5 μm with 0.25-μm step sizes.

Image analysis. The image that best captured the basal surface focal adhesion plane was chosen for analysis after deconvolving the image stacks (VayTek, Fairfield, IA). Custom image analysis algorithms for segmenting individual focal adhesion sites and tracking the corresponding translocation vectors were written for MATLAB (Math Works, Natick, MA). Translocation vectors were calculated with respect to the initial bead position, which typically did not displace more than ~1 μm.

Magnetic trap force application. The magnetic trap generated both a steady and nonreversing sinusoidal shear force of varying frequency. The steady load was applied at 0.90, 1.45, and 2.25 nN force levels, whereas the nonreversing sinusoidal forcing functions maintained a mean of 1.45 with a 2.25 nN maximum force and were applied at frequencies of 0.1, 1.0, 10, and 50 Hz. The magnetic trap force levels were calibrated by suspending the experimental magnetic beads in dimethylpolysiloxane (12 M; Sigma) and monitoring the local bead velocity as the bead moved toward the magnetic trap. With the use of Stoke's Law for viscous drag force (F) around a sphere, $F = 6 \pi \mu r V$, where μ is the fluid viscosity, r is the sphere radius, and V is the sphere velocity, the magnetic trap force generation was calibrated. For more information regarding the magnetic trap design and use refer to Huang et al. (25).

Computational simulations. Our viscoelastic, finite element model of the cell was extended to incorporate variable basal surface contact conditions mimicking the typical focal adhesion plane topology observed in our experiments. The simulation assumed a continuum, incompressible, homogeneous, isotropic Maxwell viscoelastic material with a shear modulus (G) of 100 Pa and viscosity (μ) of 100 Pa·s (characteristic time constant, $\tau = 1$ s) (28). A continuum approach effectively models large-scale cellular deformation distributions that exceed the length scales of individual microstructural cytoskeleton constituents without specifically assigning material properties for actin filaments and microtubules or accounting for the inhomogeneity observed by others (24). This continuum-like behavior has been verified experimentally by Karcher et al. (28). Geometrically the cell was modeled as a 20-μm radius half cylinder, either 5 or 3 μm high. A ramp force reaching 1.125 nN, half of the 2.25 nN experimental load, was applied to the apical cell surface over a period of 0.2 s. Initial simulations used a 5-μm height and constrained the entire basal cell surface in all three translational directions. Subsequent simulations were modified to better represent experimental adhesion conditions by correlating specific sets of model nodes on the basal cell surface to experimental regions of focal contact, fixing the focal adhesion site-associated nodes, and reducing the model height to 3 μm. The remaining basal surface nodes were free to translate. For simulation purposes, it was assumed that focal adhesion sites undergo negligible translocation during the 0.2-s simulation.

Statistical analysis. All data reported were collected from at least three separate experiments and reported as means ± SE. Differences among experimental parameters were assessed by using one- and two-way ANOVA. Post hoc paired comparisons were also performed

with the Bonferroni test (Prism 4.0; GraphPad Software, San Diego, CA). Differences were accepted as significant for P values < 0.05. Absence of a comparison bar in data figures indicates a significant data comparison with baseline.

RESULTS

GFP-paxillin expression verified with Western blot analysis. Cells infected with GFP-paxillin expressed both endogenous paxillin and exogenous GFP-paxillin. Paxillin, a 68-kDa protein, has a molecular mass of 95 kDa when fused with GFP. Western blot analysis was performed with both anti-paxillin and anti-GFP antibodies on samples containing only endogenous paxillin, endogenous paxillin plus GFP-fascin, and endogenous paxillin plus GFP-paxillin to verify the expression of GFP-paxillin. All samples expressed the 68-kDa endogenous paxillin, and cells infected with GFP-paxillin expressed the 95-kDa GFP-paxillin (Fig. 1*A*). Western blot analysis with a GFP primary antibody was performed to confirm that the anti-paxillin antibody did not associate with GFP. Only samples containing GFP-fascin and GFP-paxillin yielded positive results, indicating that GFP-paxillin was expressed (Fig. 1*B*). The phase contrast image in Fig. 1*C* corresponds to the fluorescent image in Fig. 1*D* taken 24 h posttransfection. These images show the relative transfection efficiency using GFP-paxillin.

Load magnitude affects focal adhesion translocation. Postprocessing image enhancement and analysis algorithms provided a qualitative approach to characterizing focal adhesion translocation in the presence of an externally applied force. Focal adhesion translocation was visualized by assigning single colors to fluorescent images taken at separate time points and merging the two images for comparison. Initial images ($t = 0$ min) were designated green, and subsequent images were designated red. The use of this technique enabled visualization of focal adhesion translocation for both nonspecific migratory movement, as in control experiments, and force-induced translocation. Images merged after 5 min of applying 0.90 and 2.25 nN steady loads to the apical cell surface show basal surface focal adhesion movement in response to external force application (see Fig. 2, *A* and *C*). The white arrows indicate the magnetic bead position and direction of force application. Focal adhesion visualization was further enhanced with background correction and segmentation image processing techniques, which resulted in binary equivalents to Fig. 2, *A* and *C* (see Fig. 2, *B* and *D*, respectively). Qualitatively, a 2.25 nN external steady load applied to the cell apex via cytoskeleton-connected integrins produced greater focal adhesion translocations compared with a 0.90 nN steady load (compare Fig. 2, *C* and *D* with *A* and *B*). The most evident differences between these steady loads occurred in regions local to the point of load application.

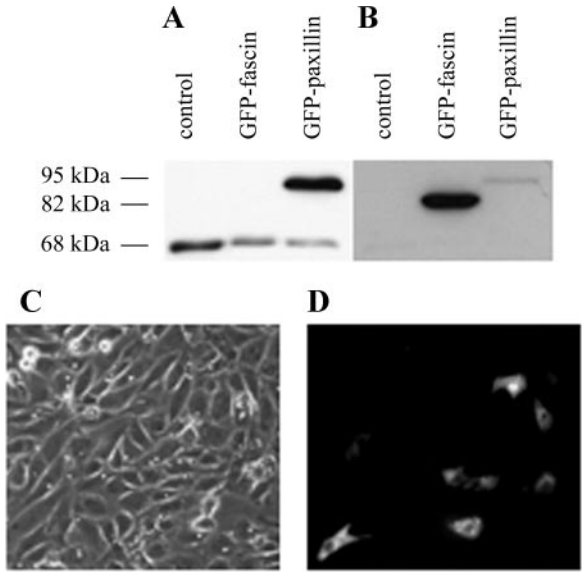

Fig. 1. Western blot analysis verification of GFP-paxillin expression using anti-paxillin (*A*) and anti-GFP (*B*). Cells transfected with GFP-paxillin expressed both endogenous paxillin (68 kDa) and exogenous GFP-paxillin (95 kDa). Comparison of the same viewing field with phase contrast imaging (*C*) and fluorescent imaging (*D*) shows the transfection efficiency.

Quantitative analysis of loading effects. The translocation of individual focal adhesion sites was quantified by calculating the centroid displacement vector between two time points. Quantitative analysis of the basis of the average length of centroid displacement vectors shows that the magnitude and frequency of load delivery, as well as the spatial position of focal adhesion sites with respect to the point load, affect focal adhesion activation and mechanosensing.

Translocation values for the control group were measured from the same cells used in forcing experiments before applying the external load. Each cell contained a single fibronectin-coated magnetic bead bound to its apical surface. The translocation magnitudes calculated for this control group were compared with the force-induced translocations. A second control group tested the potential effects of the magnetic field and local temperature elevation on focal adhesion dynamics. These control cells had single fibronectin-coated polystyrene beads bound to their apical cell surface to maintain consistency with the unforced control group. Comparison of the unperturbed and magnetic field exposed control cells confirmed that the magnetic trap had negligible effects on focal adhesion translocation (Fig. 3).

Steady load mechanotransduction threshold. Focal adhesion translocation calculated at 1, 3, and 5 min during a 0.90-nN load application did not differ from control-cell translocations. Increasing the steady load to 1.45 nN, however, yielded a significant increase in translocation. Translocation values at 1.45 and 2.25 nN were not significantly different, suggesting a threshold response level between 0.90 and 1.45 nN with little further change above the threshold (Fig. 4, *A–C*).

The mechanosensing response observed for steady loads above 0.90 nN did not occur uniformly throughout the cell. Rather, translocations tended to decrease with increasing distance from the point of load application. This observation suggests that forces transmit nonuniformly to the basal cell surface and that cells contain isolated mechanosensors capable of recognizing local force levels. To quantify this effect, translocation was examined as a function of distance from the point of load application. For lack of a better convention, the local stress concentration region was estimated from a finite element model of magnetocytometry developed in our laboratory (28) and defined as a region <7.5 μm (radially) from the projected point of load application. The global region encompassed the remainder of the cell. No spatial difference in focal adhesion translocation was observed with the 0.90-nN load

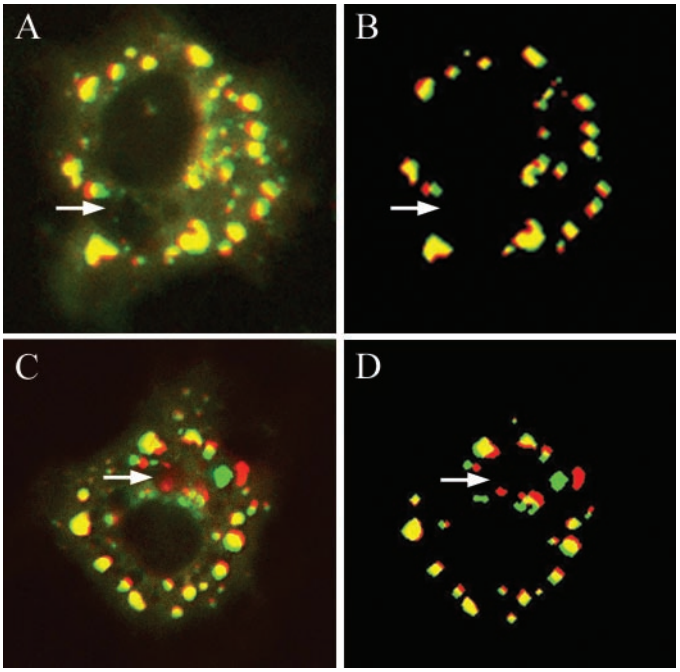

Fig. 2. Merged focal adhesion translocation images provide visualization of focal adhesion translocation where green corresponds to $t = 0$ min, red to $t = 5$ min, and yellow to overlapping regions after applying 0.90 nN steady loads (*A*) and 2.25 nN steady loads (*C*) to the apical cell surface. The magnetic bead location and direction of loading are marked by a white arrow. The 2.25 nN steady load resulted in noticeably greater translocations compared with the 0.90 nN steady load. This effect is particularly evident near the point of load application. Image processing improved focal adhesion contrast and segmented individual sites, as in *B* and *D*, which correspond to *A* and *C*, respectively.

when comparing local and global translocation values (Fig. 5*A*). On the other hand, comparison of local and global translocation magnitudes for a 1.45-nN steady load (Fig. 5*B*) yielded significantly greater local translocation values. Focal adhesion translocation in the global region still significantly exceeded the control translocations.

Finite element simulations correlating basal surface contact regions with experimental focal adhesion sites (Fig. 6*A*) provided estimates of force transmission and shear stress distribution among basal surface focal adhesion sites. The focal adhesion site-associated nodes were fixed, whereas the remaining basal surface nodes were free to displace (Fig. 6*B*). Shear forces transmitted nonuniformly to the basal contact surface with shear stress along the basal cell surface decaying with

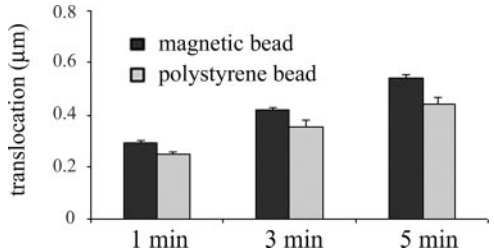

Fig. 3. Baseline focal adhesion translocation was quantified for cells binding single magnetic or polystyrene beads coated with fibronectin. The magnetic bead control ($n = 31$ cells) established a baseline for unforced focal adhesion translocation, whereas the polystyrene control ($n = 4$ cells) showed a negligible contribution of the magnetic field on focal adhesion translocation.

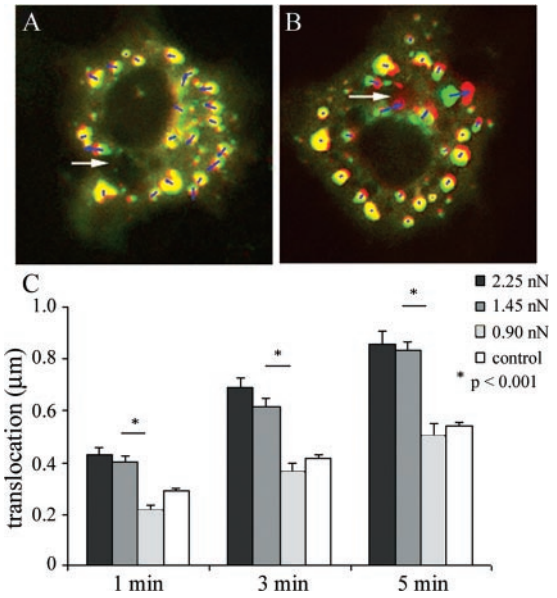

Fig. 4. Focal adhesion displacement vectors after 5 min of 0.90 nN steady loading (*A*) and 2.25 nN steady loading (*B*). The magnitude of these vectors provided a quantitative comparison of focal adhesion activation in response to external force. *C*: a significant increase in translocation was found between 0.90 ($n = 4$ cells) and 1.45 nN ($n = 8$ cells) steady load application, defining a 1.45 nN load magnitude threshold for mechanotransduction at focal adhesion sites ($^*P < 0.001$ for all time points). An insignificant difference between 2.25 ($n = 9$ cells) and 1.45 nN implies that the threshold is not graded.

distance from the point load (Fig. 6*C*). These stress distribution estimates for steady force magnetocytometry along with experimental data showing increased translocation in regions local to the point of load application provide further evidence that focal adhesion sites may function as individual mechanosensors responding to local levels of force.

Mechanotransduction depends on loading frequency. Viscoelastic cell behavior affects how local forces transmit from the cell apex and distribute among focal adhesion contact points due to the cellular relaxation times. Effects of this behavior were examined by performing excitation frequency experiments with 0.1, 1.0, 10, and 50 Hz nonreversing sinusoidal forcing functions. All sinusoidal forcing functions contained a mean positive offset force of 1.45 nN, equivalent to the smallest steady load found to activate focal adhesion sites, a maximum force of 2.25 nN, and a minimum force of 0.75 nN. A force level centered at the threshold value was selected to accentuate the frequency dependence.

Comparison of local and global translocation magnitudes, as defined previously by a 7.5-μm radius, revealed that none of the sinusoidal forcing functions, regardless of frequency, resulted in local region translocations that exceeded global translocations. Furthermore, the local translocation values resulting from the steady 1.45-nN load significantly exceeded the local values for 1.0 and 0.1 Hz loading (Fig. 7). The global translocations associated with 10 and 50 Hz forcing functions were comparable in magnitude to the steady load global translocation, whereas the 0.1 Hz forcing function produced slightly smaller translocations. Translocations associated with 1.0 Hz forcing were not significantly different than baseline translocations. Comparing the high frequency (10 and 50 Hz) forcing results to the steady load results suggests that cells transmit and

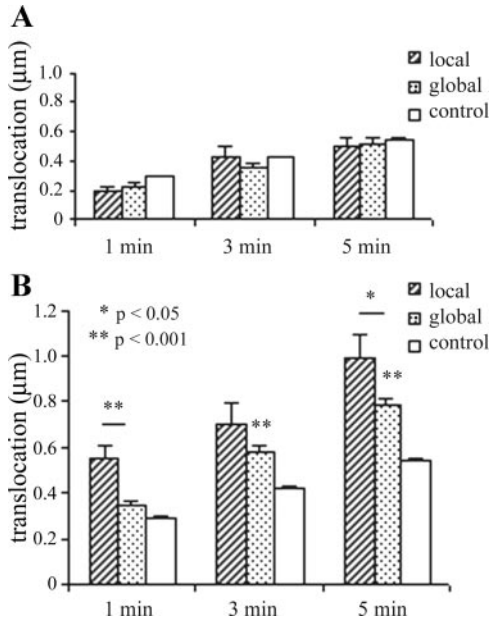

Fig. 5. A local force transmission region was defined for focal adhesion sites positioned < 7.5 μm from the projected point of load application. Focal adhesion sites outside of the local region were considered in the global region. *A*: no significant difference in local and global translocation was observed for a 0.90-nN steady load. *B*: for a 1.45-nN steady load, however, local translocation exceeded global, whereas global exceeded the unforced baseline after 5 min of loading (*$P < 0.05$ for 5 min local vs. global; **$P < 0.001$ for 1 min local vs. global, 3 min global vs. control, and 5 min local vs. global; $n = 8$ cells).

transduce oscillating forces differently compared with steady forces.

Role of tyrosine kinase activity in focal adhesion mechanotransduction. Tyrosine kinase inhibitors were applied to assess the role of the tyrosine kinase activity in force-induced focal adhesion translocation. Unforced baseline translocation levels were established by monitoring translocation before applying the magnetic field. Applying PP2, a specific Src family kinase

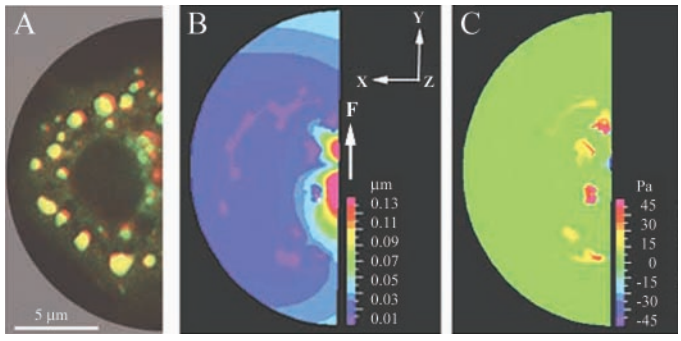

Fig. 6. A continuum, viscoelastic, finite element simulation representing experimental cell contact sites on the basal cell surface estimated the focal adhesion shear stress distribution during magnetocytometry. *A*: merged experimental fluorescent images were used to correlate focal adhesion sites to model nodes. The nodes corresponding to focal adhesion sites were fixed, and the remaining nodes were free to translate. Results of the simulation show zero displacement at focal adhesion site-associated nodes (*B*) and concentrated shear stress in focal adhesion sites near the point of load application (*C*). An external load of 1.125 nN, half of the experimental 2.25 nN due to the half-cell geometry, was applied at that midpoint of the vertical edge in the positive *y*-direction. F, force.

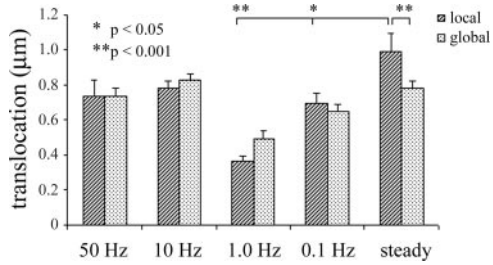

Fig. 7. Focal adhesion translocation, both locally and globally, depends on the frequency of loading. A 1.45-nN mean positive force sinusoidal wave was applied at 0.1, 1.0, 10, and 50 Hz. Local translocation in response to 5-min steady loading significantly exceeded the local translocation for 1.0 Hz (**$P < 0.001$, $n = 5$ cells) and 0.1 Hz (*$P < 0.05$, $n = 8$ cells) sinusoidal loading but not high frequency 10 Hz ($n = 9$ cells) and 50 Hz loading ($n = 5$ cells). As previously shown, steady loading yielded a significant difference between local and global responses, whereas the time-varying forcing functions did not. Furthermore, neither local nor global translocation in response to 1.0 Hz sinusoidal loading significantly exceeded baseline.

inhibitor that has been shown to inhibit activation and phosphorylation of FAK (36), resulted in a significant decrease in baseline translocation ($P < 0.0001$) compared with uninhibited levels. Conversely, genistein, a less specific ATP-competitive tyrosine kinase inhibitor, did not produce a significant difference between baseline translocation when applied for the same amount of time.

After 5 min of loading, tyrosine kinase inhibition differentially affected focal adhesion translocation depending on the inhibitor, forcing frequency, and focal adhesion site location with respect to the point load. Genistein reduced both the local and global response to steady loading and the local response to high frequency loading compared with unforced baseline levels of translocation (Fig. 8, *A* and *B*). PP2, on the other hand, effectively impaired translocation of global focal adhesion sites without inhibiting local focal adhesion sites from translocating significantly greater than baseline. The global translocation

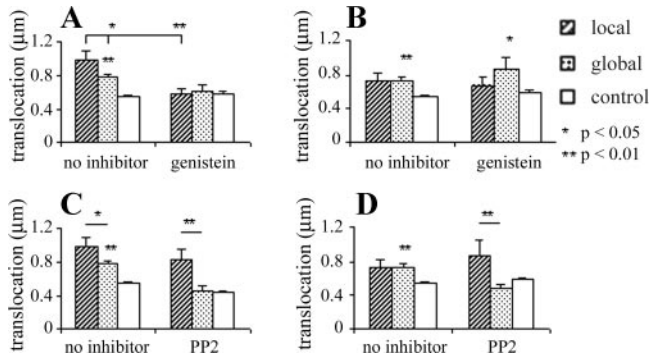

Fig. 8. Src family kinase and tyrosine phosphorylation inhibition affects local and global force-induced focal adhesion translocation after 5 min of steady and high-frequency force application. *A*: 100 μM genistein reduced the steady load translocation both locally and globally to baseline, resulting in a local response significantly less than the uninhibited local steady load translocation (**$P < 0.01$, $n = 7$ cells). *B*: however, during 50 Hz sinusoidal loading, the genistein inhibited global response still significantly exceeded baseline (*$P < 0.05$, $n = 6$ cells) without being significantly different than the 50 Hz uninhibited global response. Ten micromoles of PP2, a specific Src family kinase inhibitor, reduced global translocation to baseline for both steady (*C*) and 50 Hz (*D*) sinusoidal loading but did not impair force-induced local translocation for either forcing function (**$P < 0.01$, $n = 7$ cells for steady and $n = 4$ cells for 50 Hz; *$P < 0.05$).

after PP2 inhibition, observed for both high frequency and steady loading, was significantly less than the local translocation levels (Fig. 8, *C* and *D*). The altered levels of focal adhesion translocation resulting from tyrosine kinase and specific Src family kinase inhibition imply that force-induced focal adhesion translocation depends on force-activated kinase activity and tyrosine phosphorylation, as well as local stress distributions.

DISCUSSION

Steady load response characteristics. Force magnitude and frequency-dependent thresholds for mechanotransduction were studied by using focal adhesion dynamics as a measure of the cellular response to shear forces applied locally via adherent microbeads. On the basis of the translocation of focal adhesion sites, endothelial cells exhibit a steady force magnitude threshold for activation between 0.90 and 1.45 nN. Forces below the signal transduction threshold transmit through the cell to the basal surface without producing appreciable changes in focal adhesion translocation compared with cells not subjected to external force. Defining the level of force required to activate a specific cellular response provides critical information for studying how cells transduce external forces into biological signals. For example, molecular simulations of protein conformational changes predict pN-level force thresholds for individual proteins, whereas some ion channels require nN-level forces across the cell membrane for activation (19).

The threshold reported in this study is comparable to the total integrated shear force required to activate endothelial cells with fluid shear stress. Mechanotransduction studies with fluid shear stress typically apply stresses on the order of 1–10 dynes/cm^2 (0.1–1.0 Pa) and observe changes in intracellular calcium and nitric oxide levels (22, 27, 29, 38), ion channel activity (2, 33), G protein activation (20), gene expression (15), and focal adhesion translocation (30). This level of stress, applied over a typical endothelial cell area on the order of 1,000 μm^2, results in nN-level shear forces. Similarly, nN-level lifting forces applied normal to the apical cell surface via multiple integrin linked magnetic beads induces F-actin accumulation and tyrosine phosphorylation, increasing local membrane stiffness at the bead-membrane interface as measured with atomic force microscopy (19).

Fluid shear stress studies (38) that monitor intracellular calcium concentration changes report a stress threshold of 0.1 dynes/cm^2 for cell activation or roughly 10 pN per cell with a graded response up to 4.0 dynes/cm^2. Our results differ in both the force-level threshold and graded response findings. Focal adhesion translocation and calcium signaling likely result from two different mechanically activated biological pathways (7) and might therefore have two different activation thresholds. Furthermore, by using single bead magnetic trap loading similar to this focal adhesion translocation study did not induce a significant change in intracellular calcium compared with unforced control cells (unpublished data). These findings are consistent with previous studies indicating that calcium signaling is not an essential component to focal adhesion dynamics (13) and with data from Sawada and Sheetz (37) showing that substrate strain activates focal adhesion formation in Triton-X cytoskeletons, even in the absence of cell membranes, cytosolic-free ions, and other intracellular biomolecules.

The increased focal adhesion translocation observed at a steady load of 1.45 nN or greater did not correlate with the direction of force application after 5 min. This finding is consistent with the study of Li et al. (30), who found random focal adhesion movement during the first 10 min of fluid shear stress application. Only after ~1 h did endothelial cells subjected to fluid shear stress begin to migrate in the direction of shear force application. Furthermore, it has been shown that endothelial cells align, and actin filaments orient, with the direction of shear stress within hours of the onset of stress (3, 11). These observations suggest that the random direction of elevated focal adhesion translocation observed after 5 min of loading resulted from an unaligned actin filament organization characteristic of short loading times.

An insignificant change in focal adhesion area was observed after applying a steady mechanical load via fibronectin-coated beads, which would have presumably corresponded to the recruitment of focal adhesion proteins. Other studies have shown that external forces, applied locally with a micropipette tip (35) and optical trap (14) or globally with fluid shear stress (30) and substrate strain (37), as well as internal myosin II-driven contractile forces, modulate focal adhesion protein recruitment, which leads to focal adhesion growth (16, 45). The estimated forces required for basal surface focal adhesion growth, however, range from 3 (14) to 10 nN (35) per focal adhesion site in experiments with fibroblasts. Cells in the present study contained at least 10 focal adhesion sites per cell, which would correspond to forces per focal adhesion site one to two orders of magnitude smaller than the forces reported to induce focal adhesion recruitment and growth. These force-level comparisons suggest that focal adhesion translocation is activated with externally applied forces at significantly lower levels than required for focal adhesion reinforcement.

The details of shear force transmission from the apical cell surface to the basal surface and mechanotransduction through focal adhesions are not fully understood. It is clear, however, that externally applied forces act directly on fibronectin-bound integrins and transmit through the cytoskeleton to analogous basal surface attachments. The observed distribution of these forces among the numerous focal adhesions is quite complex and can apparently give rise to locally elevated stress levels even at locations relatively far removed from the site of forcing (24). In contrast, a continuum, viscoelastic description of the cell predicts that force levels decay with distance from a point load. Finite element analysis of magnetocytometry estimates a radial decay of force transmission through the cell to the basal surface for continuous basal surface constraints (28). The simulations performed for this study, with constrained basal surface regions corresponding to experimental focal adhesion sites, estimated that shear forces transmit nonuniformly to basal surface focal adhesion sites. The local focal adhesion sites with concentrated shear stress were shown experimentally to translocate significantly greater compared with global regions under steady loading conditions. Viscoelastic characterization of cellular force transmission would interpret this result as a direct consequence of focal adhesion sites sensing local levels of stress. However, focal adhesion sites in the global region still experienced translocations significantly greater in forced cells compared with nonforced cells, suggesting that soluble mechanosensing biomolecules, such as tyrosine ki-

nases, direct focal adhesion dynamics in peripheral cell regions.

Observations that local cell stiffness increases within minutes of applying nN-level magnetic bead forces to integrin linkages (4, 19) and Pascal-level fluid shear stress (5), provide a possible biological response mechanism for local force concentration. The formation of stress fibers could increase the local cell stiffness, elevate local force transmission, and lead to more force being supported by focal adhesion sites close to the magnetic bead. Visualization of GFP-actin, however, did not show an observable increase in local stress fiber formation after 5 min of loading (unpublished data). Consequently, the elevated focal adhesion translocation in local regions most likely did not result from the rapid formation of local stress fibers and rapid cell stiffening in response to a concentrated external force.

Focal adhesion sites appear to function as individual mechanosensors responding to local levels of external force, as supported by comparing local and global region translocation results. Other investigators report a similar sensing capability of focal adhesions in response to locally applied external forces (14, 35) as well as in response to local mechanical substrate properties (45). Internally generated actin-myosin II contraction also leads to focal adhesion activation (14, 16, 45). Two theories attempt to explain how focal adhesion sites sense local levels of force. The first recognizes that external forces locally perturb structural elements, making new binding partners more readily available. For example, tension induced integrin density increases at focal adhesion sites in coordination with focal adhesion site development and growth (1, 42). The second theory hypothesizes that external forces applied directly to structural proteins alter the protein conformational state, which transform the protein from an inactive state to an active state by exposing new binding sites (16). Both theories suggest an altered state of molecular-level equilibrium induces protein binding changes and subsequently initiates a cascade of local biological responses.

Frequency dependence of focal adhesion translocation. The experiments performed with 0.1, 1.0, 10, and 50 Hz sine wave forcing functions oscillated around a mean positive force of 1.45 nN and exhibited a biphasic cellular response with a minimum at 1.0 Hz. Frequencies greater than the maximum level were limited by the magnetic trap control capabilities. Others have reported inhibited responses of cells exposed to a near-physiological 1.0 Hz oscillating force with a positive mean compared with steady force responses (9). This frequency dependence offers a more complex view of the cellular response to external forces. For the oscillatory forcing functions, the net time during which force levels exceeded the mechanotransduction threshold did not vary with frequency nor did the minimum and maximum force levels. However, focal adhesion translocation varied with respect to the loading rate, implying that the shear force transmission distributions at the basal surface and mechanosensing signal pathways depend on the frequency of loading.

Force transmission pathways have different relaxation time constants depending on the properties of individual structural elements, and as a result, different relative strains with frequency variations. Consider the simple viscoelastic example of a parallel, two branch system where the first branch contains a single spring and the second a spring and a dashpot in series, and acknowledge extension continuity between the two branches. In the present case of constant force amplitude, extension of the isolated spring will be greatest under a steady load or at low frequencies and smallest at high frequencies. Conversely, the extension experienced by the spring in series with the dashpot will be smallest under a steady load and will increase to a constant, nonzero value at high frequencies. The transition between branch responses depends on the characteristic relaxation time of the model. If each of the two springs represents a different force transducing element within the cell, and if the system is excited near the threshold level of extension for both of these elements, then the character of the response could vary in the manner observed in our experiments. In physical terms, the two branches of this network might be on the scale of the entire cell (e.g., the cytoskeleton and the cell membrane) or on the scale of individual molecules. Others have accounted for the differential response of cellular components by modeling the viscoelastic cellular response with multiple base units in series and parallel, where each unit consists of a single spring and a spring-dashpot branch. These models show force transmission increases in branches as stiffness increases and that overall deformation decreases with increasing forcing frequency (31). The biphasic response to sinusoidal forcing functions of varying frequency may have also resulted from a combination of viscoelastic force transmission and tyrosine kinase activity, which has been shown to affect focal adhesion protein recruitment and site turnover (17, 25, 34). Although local force-induced structural changes mediated by talin 1 binding occur independently of tyrosine phosphorylation, the role of tyrosine kinases in focal adhesion mechanotransduction is not fully understood and could be partially responsible for the biphasic response observed with variable forcing frequency.

Tyrosine kinase inhibition differentially affects focal adhesion mechanotransduction. To investigate the parallel effects on focal adhesion translocation of direct force transmission and kinase signaling, tyrosine kinase activity was pharmacologically inhibited during steady and high frequency loading. Inhibition had both local and global effects that varied with the forcing function (see Fig. 8).

Applying genistein, an ATP-competitive tyrosine kinase inhibitor, impaired force-induced focal adhesion translocation both locally and globally in response to steady force application and local translocation in response to high frequency (50 Hz) loading. Although others have shown that genistein selectively impairs directed endothelial cell migration under fluid shear stress depending on the temporal variation in shear stress delivery (23), the precise effects of genistein on focal adhesion mechanotransduction remain unknown. Results from tyrosine kinase inhibition with genistein, however, do suggest that tyrosine kinase activity and tyrosine phosphorylation can differentially affect focal adhesion translocation with respect to the loading frequency.

PP2 is a more specific protein kinase inhibitor compared with genistein that inhibits Src family kinase activation and phosphorylation of FAK (36), a known upstream pathway of Rac-dependent cell migration (34). Application of PP2 reduced global focal adhesion translocation to baseline during both steady and high frequency loading but did not adversely affect local force-induced translocation. PP2 has previously been shown to affect cell motility by blocking biochemically in-

duced focal adhesion translocation (40). Furthermore, it is known that Src family kinase recruitment to FAK leads to paxillin phosphorylation and cell migration (21). Therefore, the observation that PP2 impairs global focal adhesion translocation in response to steady and high frequency loading suggests that inhibition of Src family kinase activity impairs global signaling pathways that are otherwise initiated by local force application to integrin receptors. Furthermore, in local regions of high basal shear stress where PP2 inhibition did not significantly affect translocation, the elevated focal adhesion translocation may have resulted directly from force transmission and independently of Src family kinase activity.

In summary, focal adhesion translocation resulting from mechanical stimulation has a threshold between 0.90 and 1.45 nN. The cellular response to external force depends both on the magnitude and frequency of force application. Steady load application promotes elevated local force transmission and focal adhesion translocation. At frequencies greater than the 1.0 Hz, however, loading induces focal adhesion translocation of similar magnitude in both local and global regions. Furthermore, the mechanotransduction differences between loading patterns may depend on a balanced response to mechanical force transmission and tyrosine kinase signaling. Overall these findings suggest that focal adhesion sites function as individual mechanosensors responding to local levels of force and further emphasize the intricate balance of force transmission and biochemical signaling events involved with focal adhesion mechanotransduction.

ACKNOWLEDGMENTS

We thank K. Yamada of the National Institute of Health, Bethesda, MD, for his kind gift of GFP-paxillin plasmid, and we are grateful for the technical assistance of H. Huang, J. Lammerding, P. C. Schulze, and J. Sylvan.

GRANTS

This study was supported, in part, by National Heart, Lung, and Blood Institute Grant HL-64858.

REFERENCES

1. **Ballestrem C, Hinz B, Imhof BA, and Wehrle-Haller B.** Marching at the front and dragging behind: differential αVβ3-integrin turnover regulates focal adhesion behavior. *J Cell Biol* 155: 1319–1332, 2001.
2. **Barakat AI, Leaver EV, Pappone PA, and Davies PF.** A flow-activated chloride-selective membrane current in vascular endothelial cells. *Circ Res* 85: 820–828, 1999.
3. **Barbee KA, Mundel T, Lal R, and Davies PF.** Subcellular distribution of shear stress at the surface of flow-aligned and nonaligned endothelial monolayers. *Am J Physiol Heart Circ Physiol* 268: H1765–H1772, 1995.
4. **Bausch AR, Hellerer U, Essler M, Aepfelbacher M, and Sackmann E.** Rapid stiffening of integrin receptor-actin linkages in endothelial cells stimulated with thrombin: a magnetic bead microrheology study. *Biophys J* 80: 2649–2657, 2001.
5. **Birukov BA, Dudek SM, Verin AD, Crow MT, Zhan X, DePaola N, and Garcia JG.** Shear stress-mediated cytoskeletal remodeling and cortactin translocation in pulmonary endothelial cells. *Am J Respir Cell Mol Biol* 26: 453–464, 2002.
6. **Clark CB, McKnight NL, and Frangos JA.** Strain and strain rate activation of G proteins in human endothelial cells. *Biochem Biophys Res Commun* 299: 258–262, 2002.
7. **Davies PF.** Multiple signaling pathways in flow-mediated endothelial mechanotransduction: PYK-ing the right location. *Arterioscler Thromb Vasc Biol* 22: 1755–1757, 2002.
8. **Davies PF, Barbee KA, Volin MV, Robotewskyj A, Chen J, Joseph L, Griem ML, Wernick MN, Jacobs E, Polacek DC, dePaola N, and Barakat AI.** Spatial relationships in early signaling events of flow-mediated endothelial mechanotransduction. *Annu Rev Physiol* 59: 527–549, 1997.
9. **Davies PF, Dewey CF Jr, Bussolari SR, Gordon EJ, and Gimbrone MA Jr.** Influence of hemodynamic forces on vascular endothelial function In vitro studies of shear stress and pinocytosis in bovine aortic cells. *J Clin Invest* 73: 1121–1129, 1984.
10. **Davies PF, Remuzzi A, Gordon EJ, Dewey CF Jr, and Gimbrone MA Jr.** Turbulent fluid shear stress induces vascular endothelial cell turnover in vitro. *Proc Natl Acad Sci USA* 83: 2114–2117, 1986.
11. **Davies PF, Robotewskyj A, and Griem ML.** Quantitative studies of endothelial cell adhesion. Directional remodeling of focal adhesion sites in response to flow forces. *J Clin Invest* 93: 2031–2038, 1994.
12. **Felsenfeld DP, Schwartzberg PL, Venegas A, Tse R, and Sheetz MP.** Selective regulation of integrin–cytoskeleton interactions by the tyrosine kinase Src. *Nat Cell Biol* 1: 200–206, 1999.
13. **Fleming I, Bauersachs J, Fisslthaler B, and Busse R.** Ca^{2+}-independent activation of the endothelial nitric oxide synthase in response to tyrosine phosphatase inhibitors and fluid shear stress. *Circ Res* 82: 686–695, 1998.
14. **Galbraith CG, Yamada KM, and Sheetz MP.** The relationship between force and focal complex development. *J Cell Biol* 159: 695–705, 2002.
15. **Garcia-Cardena G, Comander JI, Blackman BR, Anderson KR, and Gimbrone MA.** Mechanosensitive endothelial gene expression profiles: scripts for the role of hemodynamics in atherogenesis? *Ann NY Acad Sci* 947: 1–6, 2001.
16. **Geiger B and Bershadsky A.** Exploring the neighborhood: adhesion-coupled cell mechanosensors. *Cell* 110: 139–142, 2002.
17. **Giannone G, Jiang G, Sutton DH, Critchley DR, and Sheetz MP.** Talin1 is critical for force-dependent reinforcement of initial integrin-cytoskeleton bonds but not tyrosine kinase activation. *J Cell Biol* 163: 409–419, 2003.
18. **Gimbrone MA Jr.** Endothelial dysfunction, hemodynamic forces, and atherosclerosis. *Thromb Haemost* 82: 722–726, 1999.
19. **Glogauer M, Arora P, Yao G, Sokholov I, Ferrier J, and McCulloch CA.** Calcium ions and tyrosine phosphorylation interact coordinately with actin to regulate cytoprotective responses to stretching. *J Cell Sci* 110: 11–21, 1997.
20. **Gudi SR, Clark CB, and Frangos JA.** Fluid flow rapidly activates G proteins in human endothelial cells. Involvement of G proteins in mechanochemical signal transduction. *Circ Res* 79: 834–839, 1996.
21. **Hanks SK, Ryzhova L, Shin NY, and Brabek J.** Focal adhesion kinase signaling activities and their implications in the control of cell survival and motility. *Front Biosci* 8: d982–d996, 2003.
22. **Helmlinger G, Berk BC, and Nerem RM.** Calcium responses of endothelial cell monolayers subjected to pulsatile and steady laminar flow differ. *Am J Physiol Cell Physiol* 269: C367–C375, 1995.
23. **Hsu PP, Li S, Li YS, Usami S, Ratcliffe A, Wang X, and Chien S.** Effects of flow patterns on endothelial cell migration into a zone of mechanical denudation. *Biochem Biophys Res Commun* 285: 751–759, 2001.
24. **Hu S, Chen J, Fabry B, Numaguchi Y, Gouldstone A, Ingber DE, Fredberg JJ, Butler JP, and Wang N.** Intracellular stress tomography reveals stress focusing and structural anisotropy in cytoskeleton of living cells. *Am J Physiol Cell Physiol* 285: C1082–C1090, 2003.
25. **Huang H, Dong CY, Kwon HS, Sutin JD, Kamm RD, and So PT.** Three-dimensional cellular deformation analysis with a two-photon magnetic manipulator workstation. *Biophys J* 82: 2211–2223, 2002.
26. **Ingber DE.** Tensegrity II. How structural networks influence cellular information processing networks. *J Cell Sci* 116: 1397–1408, 2003.
27. **Jow F and Numann R.** Fluid flow modulates calcium entry and activates membrane currents in cultured human aortic endothelial cells. *J Membr Biol* 171: 127–139, 1999.
28. **Karcher H, Lammerding J, Huang H, Lee RT, Kamm RD, and Kaazempur-Mofrad MR.** A three-dimensional viscoelastic model for cell deformation with experimental verification. *Biophys J* 85: 3336–3349, 2003.
29. **Kuchan MJ and Frangos JA.** Role of calcium and calmodulin in flow-induced nitric oxide production in endothelial cells. *Am J Physiol Cell Physiol* 266: C628–C636, 1994.
30. **Li S, Butler P, Wang Y, Hu Y, Han DC, Usami S, Guan JL, and Chien S.** The role of the dynamics of focal adhesion kinase in the mechanotaxis of endothelial cells. *Proc Natl Acad Sci USA* 99: 3546–3551, 2002.
31. **Mazzag BM, Tamaresis JS, and Barakat AI.** A model for shear stress sensing and transmission in vascular endothelial cells. *Biophys J* 84: 4087–4101, 2003.

32. **Miyamoto S, Teramoto H, Coso OA, Gutkind JS, Burbelo PD, Akiyama SK, and Yamada KM.** Integrin function: molecular hierarchies of cytoskeletal and signaling molecules. *J Cell Biol* 131: 791–805, 1995.
33. **Nakao M, Ono K, Fujisawa S, and Iijima T.** Mechanical stress-induced Ca^{2+} entry and Cl^{-} current in cultured human aortic endothelial cells. *Am J Physiol Cell Physiol* 276: C238–C249, 1999.
34. **Parsons JT, Martin KH, Slack JK, Taylor JM, and Weed SA.** Focal adhesion kinase: a regulator of focal adhesion dynamics and cell movement. *Oncogene* 19: 5606–5613, 2000.
35. **Riveline D, Zamir E, Balaban NQ, Schwarz US, Ishizaki T, Narumiya S, Kam Z, Geiger B, and Bershadsky AD.** Focal contacts as mechanosensors: externally applied local mechanical force induces growth of focal contacts by an mDia1-dependent and ROCK-independent mechanism. *J Cell Biol* 153: 1175–1186, 2001.
36. **Salazar EP and Rozengurt E.** Bombesin and platelet-derived growth factor induce association of endogenous focal adhesion kinase with Src in intact Swiss 3T3 cells. *J Biol Chem* 274: 28371–28378, 1999.
37. **Sawada Y and Sheetz MP.** Force transduction by Triton cytoskeletons. *J Cell Biol* 156: 609–615, 2002.
38. **Shen J, Luscinskas FW, Connolly A, Dewey CF Jr, and Gimbrone MA, Jr.** Fluid shear stress modulates cytosolic free calcium in vascular endothelial cells. *Am J Physiol Cell Physiol* 262: C384–C390, 1992.
39. **Shen J, Luscinskas FW, Gimbrone MA Jr, and Dewey CF Jr.** Fluid flow modulates vascular endothelial cytosolic calcium responses to adenine nucleotides. *Microcirculation* 1: 67–78, 1994.
40. **Shikata Y, Birukov KG, Birukova AA, Verin A, and Garcia JG.** Involvement of site-specific FAK phosphorylation in sphingosine-1 phosphate- and thrombin-induced focal adhesion remodeling: role of Src and GIT. *FASEB J* 17: 2240–2249, 2003.
41. **Shimokawa H.** Primary endothelial dysfunction: atherosclerosis. *J Mol Cell Cardiol* 31: 23–37, 1999.
42. **Shyy JY and Chien S.** Role of integrins in endothelial mechanosensing of shear stress. *Circ Res* 91: 769–775, 2002.
43. **Traub O and Berk BC.** Laminar shear stress: mechanisms by which endothelial cells transduce an atheroprotective force. *Arterioscler Thromb Vasc Biol* 18: 677–685, 1998.
44. **White CR, Dusserre N, and Frangos JA.** Mechanotransduction in endothelial and inflammatory cells. In: *Molecular Basis for Microcirculation Disorders*, edited by Schmid-Schonbein GW. New York: Springer-Verlag, 2003, p. 640.
45. **Zamir E, Katz M, Posen Y, Erez N, Yamada KM, Katz BZ, Lin S, Lin DC, Bershadsky A, Kam Z, and Geiger B.** Dynamics and segregation of cell-matrix adhesions in cultured fibroblasts. *Nat Cell Biol* 2: 191–196, 2000.